1521-009X/44/9/1441–1449$25.00
Drug Metabolism and Disposition

http://dx.doi.org/10.1124/dmd.116.070938
Drug Metab Dispos 44:1441–1449, September 2016

Arylsulfatase B Mediates the Sulfonation-Transport Interplay in Human Embryonic Kidney 293 Cells Overexpressing Sulfotransferase 1A3[S]

Mengjing Zhao, Shuai Wang, Feng Li, Dong Dong, and Baojian Wu

Division of Pharmaceutics, College of Pharmacy, Jinan University, Guangzhou, China (M.Z., S.W., B.W.); and Ocular Surface Research Center and Institute of Ophthalmology, Jinan University School of Medicine, Guangzhou, China (F.L., D.D.)

Received April 10, 2016; accepted June 17, 2016

ABSTRACT

Elucidating the intricate relationships between metabolic and transport pathways contributes to improved predictions of in vivo drug disposition and drug-drug interactions. Here we reported that inhibited excretion of conjugative metabolites [i.e., hesperetin 3′-*O*-sulfate (H3′S) and hesperetin 7-*O*-sulfate (H7S)] by MK-571 led to reduced metabolism of hesperetin (a maximal 78% reduction) in human embryonic kidney 293 cells overexpressing sulfotransferase 1A3 (named SULT293 cells). The strong dependence of cellular sulfonation on the efflux transport of generated sulfated metabolites revealed an interplay of sulfonation metabolism with efflux transport (or sulfonation-transport interplay). Polymerase chain reaction (PCR) and Western blot analyses demonstrated that SULT293 cells expressed multiple sulfatases such as arylsulfatase A (ARSA), ARSB, and ARSC. Of these three desulfonation enzymes, only ARSB showed significant activities toward hesperetin sulfates. The intrinsic clearance values for the hydrolysis of H3′S and H7S were estimated at 0.6 and 0.5 μl/h/mg, respectively. Furthermore, knockdown of ARSB attenuated the regulatory effect of efflux transporter on cellular sulfonation, whereas overexpression of ABSB enhanced the transporter effect. Taken together, the results indicated that ARSB mediated the sulfonation-transport interplay in SULT293 cells.

Introduction

Metabolism (biotransformation) mediated by drug-metabolizing enzymes (DMEs) is an important route of drug elimination. A large portion (>70%) of marketed drugs and new chemical entities undergo extensive metabolism in vivo (Benet, 2013). Cytosolic sulfotransferases (SULTs), a class of phase II DMEs, catalyze the sulfonation (also known as sulfation) reaction, wherein a sulfonic acid is conjugated to the substrates (Chapman et al., 2004). In general, the addition of a sulfonic acid group inactivates the drug molecule and facilitates its excretion from the body. In addition to their roles in drug metabolism and detoxification, SULTs have been implicated in the activity regulation of hormones (e.g., estradiol) and neurotransmitters (e.g., dopamine) (Falany and Falany, 2007; Hempel et al., 2007). Human SULTs are divided into the following four families: SULT1, SULT2, SULT4, and SULT6 (Blanchard et al., 2004; Freimuth et al., 2004). SULT1 and SULT2 enzymes (with a total of 12 members) are well characterized and are the main contributors to chemical sulfonation (Allali-Hassani et al., 2007).

Drug transporters are the membrane proteins that facilitate the transport of drug/metabolite molecules across cell membranes, thereby regulating their body distribution. However, drug transporters (e.g., P-glycoprotein) also play an important role in determining cellular metabolism by controlling drug exposure to the enzymes (e.g., cytochrome p450 3A) (Benet, 2009; Pang et al., 2009). The dependence of drug metabolism on transporters is termed "transporter-enzyme interplay" (Benet et al., 2003; Salphati, 2009). A better understanding of transporter-enzyme interplay contributes to improved predictions of in vivo drug disposition and drug-drug interactions (Benet et al., 2003; Lam et al., 2006). In addition to P-glycoprotein/cytochrome p450 3A, the interplay is also applicable to the efflux transporters (i.e., breast cancer resistance protein and MRPs) and phase II enzymes (Jiang et al., 2012; Zhang et al., 2015). The dependence of phase II metabolism on efflux transporters is underpinned by the fact that the hydrophilic phase II metabolites (lacking in passive transport ability) require the efflux transporters for cellular excretion (Wu, 2012). The futile recycling (i.e., β-glucuronidase–mediated deglucuronidation) has been suggested to be the main mechanism underlying the glucuronidation-transport interplay (Sun et al., 2015b). In contrast to the well-established interplay of

This work was supported by the National Natural Science Foundation of China [Grant 81573488], the Young Scientist Special Projects in biotechnological and pharmaceutical field of 863 Program [Grant 2015AA020916], the Outstanding Youth Fund from the Natural Science Foundation of Guangdong Province [Grant 2014A030306014], and The PhD Start-up Fund of Natural Science Foundation of Guangdong Province [Grant 2015A030310339].

M.Z. and S.W. contributed equally to this work.

dx.doi.org/10.1124/dmd.116.070938.

[S]This article has supplemental material available at dmd.aspetjournals.org.

ABBREVIATIONS: ARSA, arylsulfatase A; ARSB, arylsulfatase B; ARSC, arylsulfatase C; CL_{int}, intrinsic clearance; DME, drug-metabolizing enzyme; DMEM, Dulbecco's modified Eagle's medium; FBS, fetal bovine serum; f_{met}, fraction of drug metabolized; GAPDH, glyceraldehyde-3-phosphate dehydrogenase; HEK, human embryonic kidney; H7S, hesperetin 7-*O*-sulfate; H3′S, hesperetin 3′-*O*-sulfate; MRP, multidrug resistance-associated protein; MS, mass spectrometry; PCR, polymerase chain reaction; QTOF, quadrupole time of flight; qPCR, quantitative polymerase chain reaction; RT-PCR, reverse transcription-polymerase chain reaction; shARSB, short hairpin RNA sequence targeting arylsulfatase B; shRNA, short hairpin RNA; SULT, sulfotransferase, UPLC, ultraperformance liquid chromatography.

glucuronidation with efflux transport, little is known about whether and how the sulfonation-transport interplay occurs.

Desulfonation refers to the hydrolysis of sulfate esters in which the sulfate conjugate is converted back to the parent compound (Hanson et al., 2004). The desulfonation reaction is catalyzed by the sulfatase family of enzymes. Human sulfatases consist of 17 enzymes that have different locations (Hanson et al., 2004; Diez-Roux and Ballabio, 2005). They are located in lysosome [arylsulfatase A (ARSA), ARSB, iduronate 2-sulfatase, heparan *N*-sulfatase, *N*-acetylglucosamine-6-sulfatase, *N*-acetyl-galactosamine-6-sulfatase, and telethon sulfatase], endoplasmic reticulum [ARSC, ARSD, ARSF, ARSG, ARSH, ARSJ, and ARSK], Golgi apparatus (ARSE), or cell surface (sulfatase 1 and sulfatase 2) (Diez-Roux and Ballabio, 2005). Sulfatases use the formylglycine (derived from a cysteine) as the catalytic residue that attacks the sulfur atom upon activation by a water molecule (Ghosh, 2007). Due to their roles in the regulation of cell metabolism and signaling, genetic deficiencies of sulfatases result in various pathophysiological conditions such as hormone-dependent cancers, lysosomal storage disorders, and developmental abnormalities (Hanson et al., 2004; Buono and Cosma, 2010). Although the biologic functions of sulfatases are becoming clearer, the role of sulfatases in the disposition of drug/metabolite molecules remained underexplored.

Hesperetin, a natural flavonoid found in citrus fruits, has various pharmacological activities, such as anticancer and cardiovascular protective effects (Garg et al., 2001; Roohbakhsh et al., 2015). Hesperetin is extensively metabolized by phase II enzymes to form sulfate and glucuronide conjugates, resulting in exceedingly low bioavailability after oral administration (Brand et al., 2008, 2010). Recent studies have indicated that phase II conjugates of hesperetin retain the biologic activities of the parent molecule (Takumi et al., 2012; Yang et al., 2012). This helps to explain why oral hesperetin has in vivo activities despite the fact that the compound is the least bioavailable (Giménez-Bastida et al., 2016). Therefore, it assumes great importance to understand the disposition mechanisms of both hesperetin and its conjugative metabolites in an attempt to developing hesperetin as a therapeutic agent.

The transporter-enzyme interplay remains undefined for the SULT-MRP pair. In our previous studies, we have shown that MRP4 is primarily involved in the efflux transport of flavonoid sulfates [including hesperetin 7-*O*-sulfate (H7S) and hesperetin 3′-*O*-sulfate (H3′S)] in SULT1A3-overexpressing human embryonic kidney (HEK) 293 cells (also called SULT293 cells) (Li et al., 2015; Sun et al., 2015a). In the present study, we examined the sulfonation-transport interplay (or SULT1A3-MRP4 interplay) in SULT293 cells using hesperetin as a model compound. Moreover, we unraveled the important role of sulfatases in the sulfonation-transport interplay.

Materials and Methods

Materials. Recombinant ARSA and ARSB enzymes were purchased from R&D Systems (Minneapolis, MN). pLVX-PGK-Puro, pLVX-ShRNA2-Neo, and pcDNA3.1(-) vectors were obtained from BioWit Technologies (Shenzhen, China). Anti-ARSA, anti-ARSB, and anti-ARSC antibodies were purchased from OriGene Technologies (Rockville, MD). Anti–glyceraldehyde-3-phosphate dehydrogenase (GAPDH) antibody was purchased from Abcam (Cambridge, MA). MK-571 was purchased from Sigma-Aldrich (St Louis, MO). Hesperetin was purchased from Aladdin Reagents (Shanghai, China). H3′S and H7S were synthesized (used as reference standards) in our laboratory using rat liver S9 fraction.

Synthesis, Purification, and Structural Identification of Hesperetin Sulfates. Hesperetin sulfates (i.e., S1 and S2 eluted at 2.47 and 2.68 minutes in the Waters ACQUITY UPLC system; Fig. 1) were generated using rat liver S9 fraction (XenoTech LLC, Lenexa, KS). In brief, the incubation mixture of 500 ml contained the S9 fraction (final concentration: 0.5 mg total protein/ml), 3′-phosphoadenosine 5′-phosphosulfate (100 μM), and hesperetin (10 μM) in potassium phosphate buffer (50 mM, pH 7.4). After incubation for 6 hours at 37°C, ice-cold acetonitrile (50 ml) was added to terminate the reaction and to precipitate the proteins. The incubation mixture was aliquoted and centrifuged at 18,000*g* for 15 minutes. The supernatant was pooled, concentrated, and subsequently injected into the Dionex U300 HPLC System for purification. Chromatographic elution was performed with an Agilent Eclipse XDB-C18 column (5 μm, 4.6 × 250 mm) using 70% acetonitrile-0.1% formic acid in water as the mobile phase. Fractions containing S1 and S2 were respectively collected and dried in vacuo. The purities of both metabolites (about 4 mg) were >97% by high-pressure liquid chromatography-UV analysis.

Structural identification was performed through the Waters UPLC-QTOF (quadrupole time of flight)/MS (mass spectrometry) system (consisting of ACQUITY UPLC and Xevo G2 QTOF/MS, operating in the positive ion mode) and ^{1}H NMR (dimethylsulfoxide-d6) analyses. ^{1}H NMR spectra were recorded on Bruker AV-500 Spectrometer using tetramethylsilane as an internal standard. Hesperetin generated a ion $[M+H]^+$ of *m/z* 302.079 in QTOF/MS, whereas the two metabolites showed ions at *m/z* 382.036. An increase of 80 Da in mass (corresponding to a sulfonate group) indicated that the two metabolites were monosulfate conjugates. In the ^{1}H NMR spectrum, the chemical shift values (δ) of hesperetin was 6.99 ppm for H-2′. The corresponding signal for S1 was shifted downfield to 7.63 ($\Delta\delta$ = +0.64 ppm), indicating that 3′-OH position was substituted. The δ values of hesperetin were 5.92 ppm for H-6 and 5. 96 ppm for H-8. These signals were respectively changed to 6.06 ($\Delta\delta$ = + 0.14 ppm) and 6.39 ppm ($\Delta\delta$ = +0.43 ppm) in the S2 spectrum, indicating that the 7-OH position was substituted. Therefore, S1 and S2 were identified as 3′-*O*-sulfate and 7-*O*-sulfate of hesperetin, respectively.

Establishment of SULT1A3-Overexpressing HEK293 Cells. SULT1A3-overexpressing HEK293 cells (called SULT293 cells) had been established and were characterized in our laboratory (Li et al., 2015; Sun et al., 2015a).

Development of ARSC Stably Transfected HEK293 Cells. HEK293 cells were stably transfected with the cDNA of human ARSC using the lentiviral transduction approach (Quan et al., 2015). The ARSC cDNA (1752 bp) was

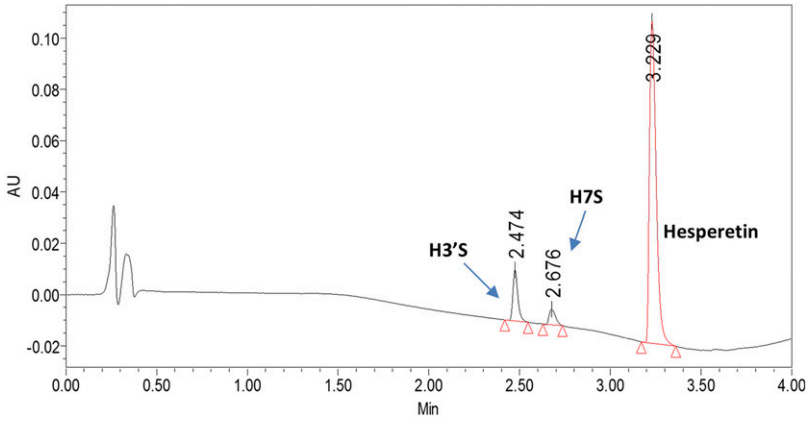

Fig. 1. Representative UPLC chromatogram for analyses of hesperetin sulfates.

TABLE 1

Primer sets for RT-PCR and qPCR

Primer	Forward (5′→ 3′Sequence)	Reverse (5′→ 3′Sequence)
ARSA	AGGCTACCTCACAGGAATG	CACCGTCGCAAGGAGT
ARSB	CATAACTAACCATCCACCAG	TGTTCCAGAGCCCACT
ARSC	ACCCTCATCTACTTCACAT	TAGTGGGCTCATCAATC
GADPH	TCTGACTTCAACAGCGACACC	CTGTTGCTGTAGCCAAATTCGT

polymerase chain reaction (PCR) amplified from the pCMV6-XL5-ARSC plasmid (OriGene Technologies). The forward and reverse primers were 5′-CGGAATTCGCCACCATGCCTTTAAGGAAGATGAAGATCC-3′ and 5′-CGGGATCCCTAGCGGCTCAGTCTCTTATCCTG-3′, respectively. The restriction sites of EcoRI and BamHI were introduced into the primers (underlined portions in the sequences). The 50-μl PCR mixture contained 10 μl of 5× FastPfu Buffer, 4 μl of 2.5 mM deoxy-NTPs, 2 μl of primers (10 μM), 1 μl of template DNA (100 ng/ml), and 1 μl FastPfu polymerase (TransGen Biotech, Beijing, China). The PCR program was set as follows: 3-minute denaturation at 95°C followed by 35 cycles of 20 seconds at 95°C, 30 seconds at 55°C, and 2 minutes at 72°C, and a final step of 72°C for 5 minutes. The PCR products were analyzed by gel electrophoresis (1% agarose), and the fragment of 1752 bp (ARSC cDNA) was collected and purified. The cDNA of ARSC was subcloned to the pLVX-PGK-Puro vector through EcoRI and BamHI restriction. The recombinant plasmid was then introduced into 293T cells by transient transduction to produce lentiviral particles. The resulting lentiviral particles were used to transduce HEK293 cells. To be specific, HEK293 cells were cultured in Dulbecco's modified Eagle's medium (DMEM) supplemented with 10% fetal bovine serum (FBS). On day 2, the culture medium was changed to pure DMEM, and the lentiviruses (multiplicity of infection = 10) were introduced. After a 2-hour transduction, the cells were maintained in DMEM with 10% FBS. On day 4, the transfected cells and untransfected cells (as a control) were cultured in DMEM containing 10% FBS and 6-μg/ml puromycin, and the medium was changed every 2 days. As all control cells died, the culture medium for transfected cells was changed to DMEM containing 10% FBS and 2-μg/ml puromycin. Once 100% confluence was reached, the cells were collected and processed for DNA identification. Stably transfected cells were obtained after continuous culture for two passages. The transduction efficiency was evaluated by measuring the ARSC protein levels in both control and transfected cells.

Transient Transduction of SULT293 Cells with ARSB. ARSB cDNA (1602 bp) was PCR amplified from the pGEM-T-ARSB plasmid (Sino Biologic Inc., Beijing, China) with forward primer of 5′-CCCTCGAGGCCACCATGGGTCCGCGCGGCGCGGCGAGCT-3′ and reverse primer of 5′-CCAAGCTTCTACATCCAAGGGCCCCACACCCCA-3′), and subcloned to the pcDNA3.1(-) vector. The recombinant plasmid or blank plasmid (as a control) was introduced into SULT293 cells using the HET kit (a modified calcium phosphate transduction reagent kit) following the manufacturer instructions (BioWit Technologies). The transduction efficiency was evaluated by measuring the ARSB protein levels in both control and transfected cells. Cells were ready for experiments 2 days after transduction.

Transient Transduction of SULT293 Cells with shRNA Targeting ARSB. The shRNA sequence targeting ARSB (shARSB) (forward: 5′-GATCC GCTATAGCCCTCATAACTAAC TTCAAGAGA GTTAGTTATGAGGGCTATAGCTTTTTTACGCGTC-3′; reverse: 5′ -TCGAGACGCGTAAAAAAGCTATAGCCCTCATAACTAACTCTCTTGAAGTTAGTTATGAGGGCTATAGCG-3′) was synthesized by BioWit Technologies. This shRNA was ligated to the pLVX-ShRNA2-Neo plasmid through BamHI and XhoI restriction. The resulting shRNA construct was used to transduce SULT293 cells. To be specific, cells were seeded at a density of 2.0×10^5 cells/well in a six-well plate and maintained at 37°C in DMEM containing 10% FBS. On the next day, the plasmid construct carrying the shARSB or scramble (forward: 5′-GATCCGCTCGCCTGTCTACTAACTAATTCAAGAGATTAGTTAGTAGACAGGCGAGCTTTTTTACGCGTC-3′; reverse: 5′-TCGAGACGCGTAAAAAAGCTCGCCTGTCTACTAACTAATCTCTTGAATTAGTTAGTAGACAGGCGAGCG-3′) (4 μg) was introduced into the cells using Polyfectine following the manufacturer protocol (BioWit Technologies). The transduction efficiency was evaluated by measuring the ARSB protein levels in both scramble and shARSB transfected cells. Cells were used for sulfate excretion experiments 2 days after shRNA transduction.

Cell Lysate Preparation. Cell lysate were prepared using the sonication method as described previously (Quan et al., 2015). In brief, the cells were collected and suspended in potassium phosphate buffer (50 mM, pH 7.4). This was followed by sonication for 15 minutes in an ice-cold water bath. Cell lysate

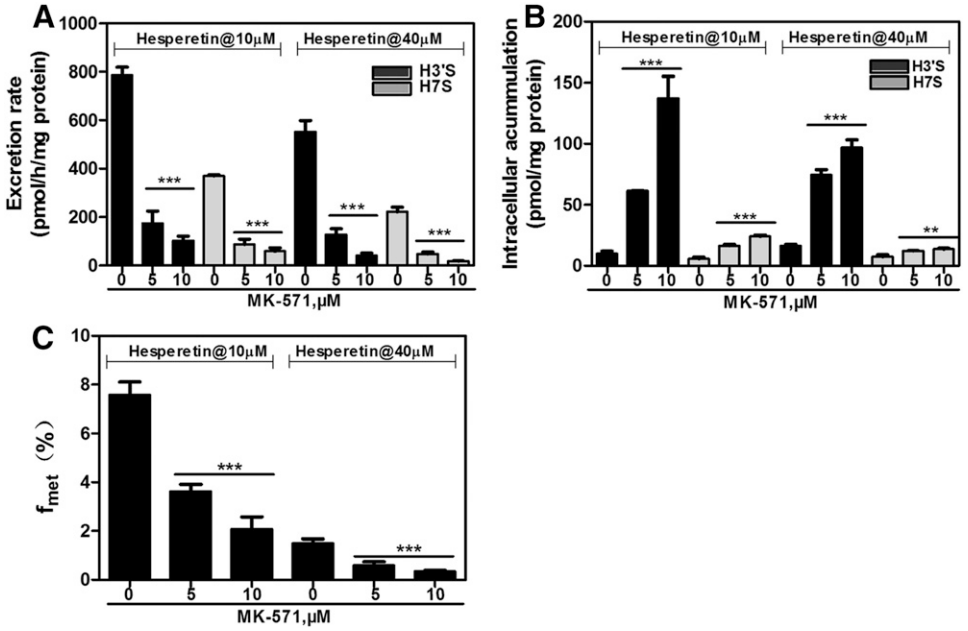

Fig. 2. Effects of MK-571 on the disposition of hesperetin sulfates after the incubation of SULT293 cells with hesperetin (10 and 40 μM). (A) Effects of MK-571 on the excretion rates of hesperetin sulfates. (B) Effects of MK-571 on the intracellular levels of hesperetin sulfates at the end of the experiment (2 hours). (C) Effects of MK-571 on total cellular metabolism (represented by the f_{met} value). Each data point was the average of the data from three independent experiments, with the error bar representing the S.D. $^{**}P < 0.01$; $^{***}P < 0.001$ compared with the control group.

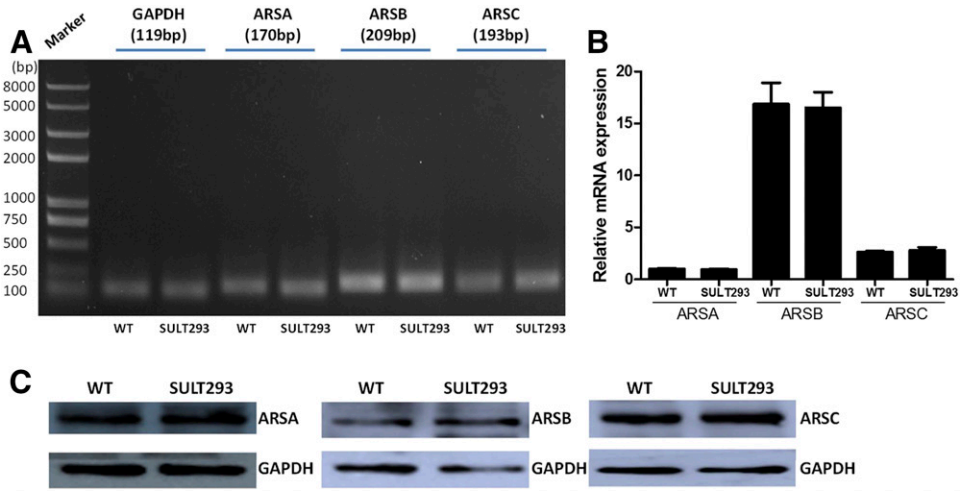

Fig. 3. Expression of sulfatases in HEK293 cells. (A) mRNA expression of three sulfatases in HEK293 and SULT293 cells detected by RT-PCR. (B) qPCR measurements of ARSA, ARSB, and ARSC in SULT293 cells. The data were generated from three independent qPCR experiments, with the error bar representing the S.D. (C) Protein expression of ARSA, ARSB, and ARSC in HEK293 and SULT293 cells. WT, wild type.

was obtained by centrifugation (4°C) at 1,000*g* for 5 minutes. Total protein concentration of cell lysate was determined using a protein assay kit (Bio-Rad, Hercules, CA).

Reverse-Transcription PCR. Cells were collected, and total RNA isolation was performed using the TRIzol extraction method. The total RNA was converted to cDNA using the iScript cDNA Synthesis Kit according to the manufacturer protocol (Bio-Rad). The PCR conditions were as follows: 3-minute denaturation at 95°C, followed by 30 cycles of 20 seconds at 95°C, 30 seconds at 55°C, and 30 seconds at 72°C, and a final step of 72°C for 5 minutes using Taq DNA polymerase (TransGen Biotech). The primer sequences are summarized in Table 1.

Quantitative Real-Time PCR. Total RNA was isolated using the TRIzol extraction method. The PCR conditions were as follows: 30 seconds of denaturation at 95°C, followed by 45 cycles of 10 seconds at 95°C, 30 seconds at 60°C, and 30 seconds at 72°C, and a final step of 1 minute at 95°C, 1 minute at 55°C, and 1 minute at 95°C. Each sample contained 0.2 μg of cDNA in 10 μl of SYBR green/fluorescein quantitative PCR (qPCR) Master Mix (Thermo Scientific, Waltham, MA) and 8 pmol of each primer in a final volume of 20 μl. The primers used for qPCR were listed in Table 1. Data were analyzed according to the $2^{-\Delta\Delta CT}$ method, and the relative amount of each studied mRNA was normalized to the level of ARSA in HEK293 cells.

Desulfonation Assay. The enzyme material (expressed ARSA, expressed ARSB, or lysate preparations) was incubated with hesperetin sulfates at 37°C to determine the potential of the sulfatase enzymes in catalyzing the sulfate hydrolysis reaction. In brief, 120 µl of the sodium acetate buffer (pH 4.6, 5.6, or 7.0) was used as the incubation medium. The enzyme material (a final concentration of 0.34 mg protein/ml) was added to the incubation buffer, followed by the addition of hesperetin sulfates. The reaction was initiated by incubation at 37°C. After a 2-hour incubation time, the reaction was stopped by adding 50 μl of ice-cold acetonitrile. The samples were centrifuged at 18,000*g* for 15 minutes, and the supernatant was analyzed by UPLC (Sun et al., 2015a). The hydrolysis activity of the ARSC enzyme was derived by subtracting the hydrolysis rate of control lysate from that of the ARSC lysate.

Sulfate Excretion Experiments. Sulfate excretion experiments were performed following our published procedures (Li et al., 2015; Sun et al., 2015a). The cells were incubated with a 2-ml dosing solution, namely, the Hanks' balanced salt solution buffer containing hesperetin (10 or 40 μM) at 37°C. MK-571, when used, was coincubated with hesperetin. This was done by diluting the MK-571 stock solution (prepared in dimethylsulfoxide) by a factor of 1:1000 with the dosing solution. At each time point (0.5, 1, 1.5, and 2 hours), a 200-μl aliquot of incubation medium was sampled and immediately replenished with the same volume of dosing solution. The samples were subjected to UPLC analyses to

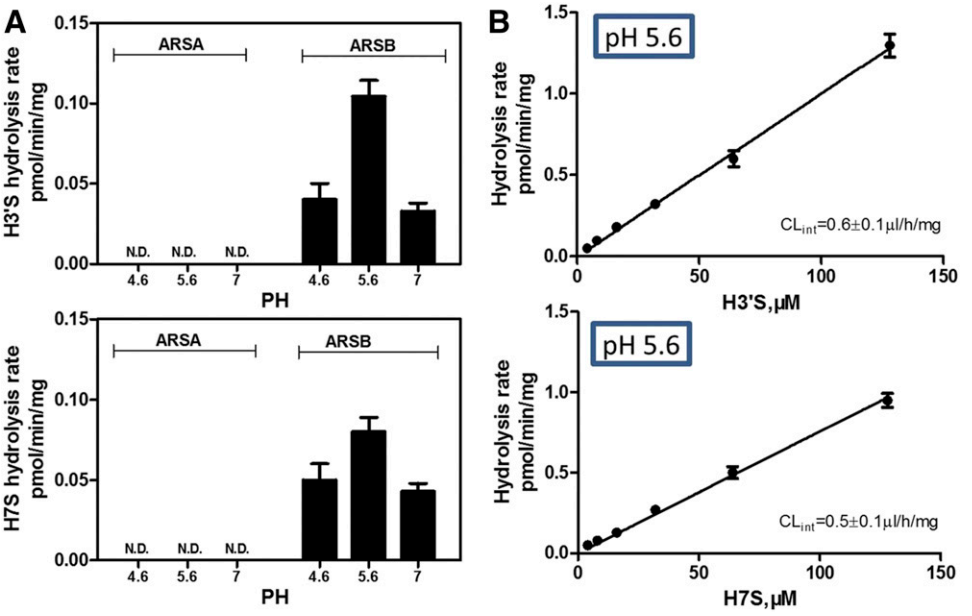

Fig. 4. Activity characterization of sulfatases ARSA and ARSB. (A) Hydrolysis activity measurements of ARSA and ARSB toward hesperetin sulfates at 8 μM. (B) Hydrolysis kinetics of hesperetin sulfates by ARSB. Each data point was the average of the activity data from three independent experiments, with the error bar representing the S.D. N.D., not detected.

determine the sulfate concentrations, as described previously (Sun et al., 2015a). After sampling at the last time point (2 hours), the cells were collected and disrupted to measure the intracellular amounts of sulfate conjugates. To be specific, the culture medium was rapidly removed by suction, and the cells were washed twice with ice-cold Hanks' balanced salt solution. Then, each culture well was solubilized with 400 μl of ice-cold MeOH:H2O (5:5, v/v) and subjected to sonication in an ice-cold ultrasonic bath for 15 minutes. The homogenate was centrifuged for 15 minutes at 18,000*g*, and the resulting supernatant was analyzed by UPLC. The excretion rate of sulfate (eq. 1) and f_{met} (fraction of drug metabolized; eq. 2) value were determined exactly as described (Quan et al., 2015; Zhang et al., 2015). The f_{met} value measures the extent of compound sulfonation (or formation of sulfate metabolites) in the cell system.

$$ER = V\frac{dC}{dt} \quad (1)$$

Where V was the volume of the incubation medium, C was the cumulative concentration of the hesperetin sulfate, and t is the incubation time. dC/dt described the changes of hesperetin sulfate levels with the time.

$$f_{met} = \frac{Excreted \text{ sulfate metabolites} + Intracelluar \text{ sulfate metabolites}}{Dosed \text{ hesperetin}} \quad (2)$$

Western Blotting. The cell lysate (30 μg of total protein) was subjected to SDS-PAGE (10% acrylamide), followed by the transfer of proteins to polyvinylidene fluoride membranes. Blots were probed with anti-ARSA (or anti-ARSB or anti-ARSC) and anti–GAPDH (as a loading control) antibodies, followed by horseradish peroxidase–conjugated rabbit anti-goat IgG. Protein bands were visualized by enhanced chemiluminescence, and band intensities were analyzed using the Quantity One software.

Quantification of Hesperetin Sulfates by UPLC. Quantification of hesperetin sulfates was performed using a Waters ACQUITY UPLC system (Waters, Milford, MA). Chromatographic elution was performed on a Kinetex C18 column (2.1 × 50 mm, 2.6 μm; Phenomenex) using a gradient of 2.5 mM ammonium acetate in water (mobile phase A) versus acetonitrile (mobile phase B) at a flow rate of 0.4 ml/min. The gradient program consisted of 10% mobile phase B at 0 to 0.5 minute, 10–30% mobile phase B at 0.5–2.0 minutes, 90% mobile phase B at 2.0–3.4 minutes, and 90–10% mobile phase B at 3.4–4 minutes. The detection wavelength was 287 nm.

Statistical Analysis. Data are expressed as the mean ± S.D. from three independent experiments. Differences among multiple groups were analyzed using one-way ANOVA followed by Dunnett's post hoc test. Differences between two groups were analyzed by Student's *t* test. The level of significance was set at $^{*}P < 0.05$, $^{**}P < 0.01$, or $^{***}P < 0.001$.

Results

Sulfonation-Transport Interplay in SULT293 Cells. The SULT293 cells generated two monosulfate conjugates (i.e., H3′S and H7S) from hesperetin (10 and 40 μM) owing to the stable expression of SULT1A3. In line with our previous study (Sun et al., 2015a), MK-571, a pan-MRP inhibitor, significantly reduced the excretion of hesperetin sulfates, leading to cellular accumulation of the metabolites (Fig. 2, A and B). Interestingly, the f_{met} value (representing the extent of total compound metabolism in the cells) was significantly decreased by MK-571 (Fig. 2C). This indicated that hesperetin metabolism was highly dependent on the efflux transport of its sulfated metabolites, a phenomenon termed "sulfonation-transport interplay." It was noted that the excreted metabolites was higher at a 10 μM dose of hesperetin compared with a 40 μM dose (Fig. 2A). This most likely was accounted for by the substrate inhibition (a lower metabolism rate at a higher substrate concentration), as observed previously (Sun et al., 2015a).

Expression and Activity Characterization of Sulfatases in HEK293 Cells. Reverse-transcription PCR (RT-PCR) showed that HEK293 cells (both wild-type and transfected) expressed mRNAs of ARSA, ARSB, and ARSC (Fig. 3A). Relative mRNA levels of the three genes were determined by qPCR. The mRNA levels of ARSB and ARSC were 16-fold and 3-fold that of ARSA, respectively (Fig. 3B). Western blotting confirmed that ARSA, ARSB, and ARSC proteins were all expressed in the cells (Fig. 3C).

The activities of ARSA and ARSB toward the sulfated metabolites were measured using their corresponding recombinant enzymes that are commercially available. ARSB showed significant hydrolysis (desulfonation) activities toward hesperetin sulfates, whereas ARSA did not (Fig. 4A). Consistent with its lysosomal location, the optimal hydrolysis pH for the ARAB enzyme was acidic (Fig. 4A). The intrinsic clearance (CL_{int}) for the hydrolysis kinetics was estimated by performing linear regression (CL_{int} equaled the slope). The ARSB enzyme possessed a similar catalytic efficiency toward the two hesperetin sulfate isomers (0.6 versus 0.5 μl/h/mg, $P > 0.05$) (Fig. 4B).

Recombinant ARSC enzyme is not available commercially. The ARSC activity herein was determined using the lysate preparations from ARSC-overexpressing HEK293 cells (ARSC) and control cells. The ARSC activity was estimated as the hydrolysis rate difference between the control lysate and ARSC lysate. Overexpression of ARSC in HEK293 cells was confirmed by Western blotting (Fig. 5A). Both

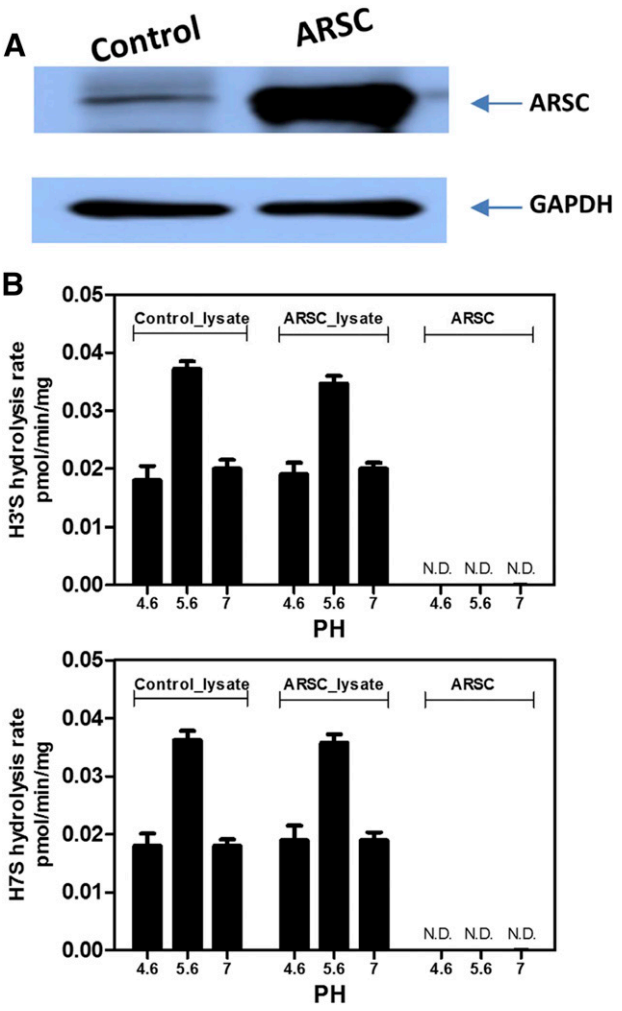

Fig. 5. Activity characterization of ARSC sulfatase. (A) Western blotting of the ARSC-overexpressing HEK293 (ARSC) and wild-type (control) cells against human ARSC. (B) Hydrolysis activity measurements of ARSC lysate and control lysate toward hesperetin sulfates at 8 μM. The hydrolysis activity of ARSC enzyme was estimated by subtracting the hydrolysis rate of control lysate from that of ARSC lysate. Each data point was the average of the activity data from three independent experiments, with the error bar representing the S.D. N.D., not detected.

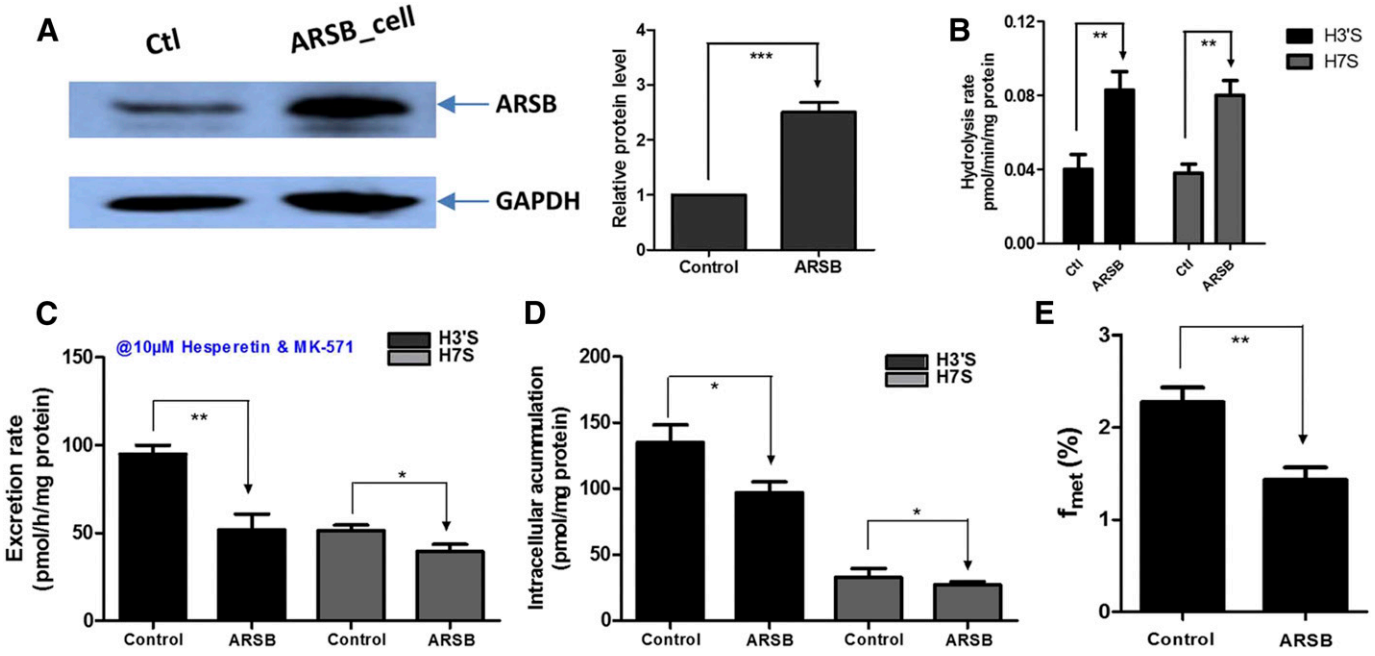

Fig. 6. Role of ARSB in the sulfonation-transport interplay. (A) Western blot analysis of ARSB in control and ARSB-overexpressing (ARSB_cell) SULT293 cells. (B) Effects of ARSB overexpression on the hydrolysis activity of the cells toward hesperetin sulfates at 8 μM. (C) The effects of ARSB overexpression on hesperetin sulfate excretion after the dosing of hesperetin and MK-571 (10 μM). (D) The effects of ARSB overexpression on hesperetin sulfate accumulation after the dosing of hesperetin and MK-571 (10 μM). (E) The effects of ARSB overexpression on total cellular sulfonation (f_{met}) after the dosing of hesperetin and MK-571 (10 μM). Each data point was the average of the data from three independent experiments, with the error bar representing the S.D. $^*P < 0.05$; $^{**}P < 0.01$; $^{***}P < 0.001$.

ARSC and control lysate showed activities toward hesperetin sulfates (Fig. 5B). However, there was no significant difference ($P > 0.05$) between the hydrolysis rates of the ARSC and control lysate, indicating that ARSC enzyme had no significant activity toward hesperetin sulfates (Fig. 5B). Further, both lysate preparations performed best at a pH of 5.6, lending strong support to the fact that ARSB was the main enzyme catalyzing the hydrolysis of hesperetin sulfates in the cells (Fig. 5B).

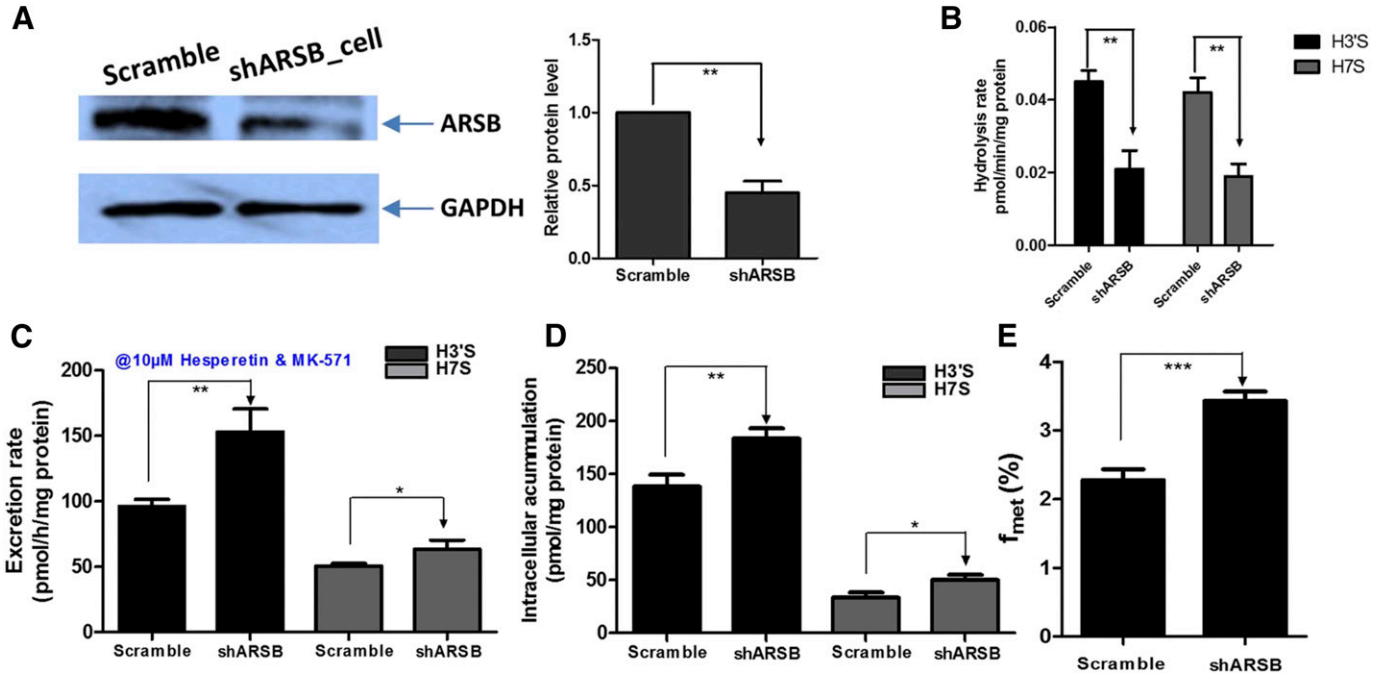

Fig. 7. Role of ARSB in the sulfonation-transport interplay. (A) Western blot analysis of ARSB in scramble and ARSB knockdown (shARSB_cell) SULT293 cells. (B) Effects of ARSB knockdown on the hydrolysis activity of the cells toward hesperetin sulfates at 8 μM. (C) The effects of ARSB silencing on hesperetin sulfate excretion after the dosing of hesperetin and MK-571 (both at 10 μM). (D) The effects of ARSB silencing on hesperetin sulfate accumulation after the dosing of hesperetin and MK-571 (both at 10 μM). (E) The effects of ARSB silencing on total cellular sulfonation (f_{met}) after the dosing of hesperetin and MK-571 (both at 10 μM). Each data point was the average of the data from three independent experiments, with the error bar representing the S.D. $^*P < 0.05$; $^{**}P < 0.01$; $^{***}P < 0.001$.

Effects of MK-571 on ARSB Activity. In vitro experiments were performed to determine the effects of the MRP inhibitor MK-571 on ARSB activity using its recombinant enzyme. MK-571 of 5–20 μM did not show any modulatory effects on ARSB-mediated hydrolysis of H3′S (Supplemental Fig. 1). Likewise, MK-571 did not alter the hydrolysis rates of H7S by ARSB (Supplemental Fig. 1). The results suggested that MK-571 would not interfere with the desulfonation process in the cells.

Role of ARSB in the Sulfonation-Transport Interplay. To determine the role of ARSB in the sulfonation-transport interplay, the protein level of ARSB in SULT293 cells was upregulated by transient transduction of ARSB or downregulated by shRNA. Upregulation and downregulation of ARSB were confirmed by Western blot analysis (Fig. 6A; Fig. 7A). Further, ARSB upregulation led to a 2.1-fold increase ($P < 0.01$) in the hydrolysis activity of the cells (Fig. 6B), whereas ARSB downregulation caused significant reductions (53.3–54.8%, $P < 0.01$) in the hydrolysis activities of the cells toward hesperetin sulfates (Fig. 7B).

In the presence of MK-571, high ARSB expression led to significant reductions in both the excretion and accumulation of hesperetin sulfates (Fig. 6, C and D). As a result, the f_{met} value was decreased (Fig. 6E). Thus, the upregulation of ARSB enhanced the transporter effect on total cellular sulfonation (reflected by f_{met}) of hesperetin (Fig. 2C; Fig. 6E). On the contrary, shRNA-mediated silencing of ARSB caused significant increases in both the excretion and accumulation of hesperetin sulfates (Fig. 7, C and D). Accordingly, the f_{met} value was increased by shARSB (Fig. 7E). Therefore, the downregulation of ARSB attenuated the transporter effect on hesperetin sulfonation in the cells (Fig. 2C; Fig. 7E). Similar results were observed at a dose of 40 μM hesperetin (Supplemental Fig. 2). The results consistently indicated that the ARSB enzyme was a key determinant to the sulfonation-transport interplay.

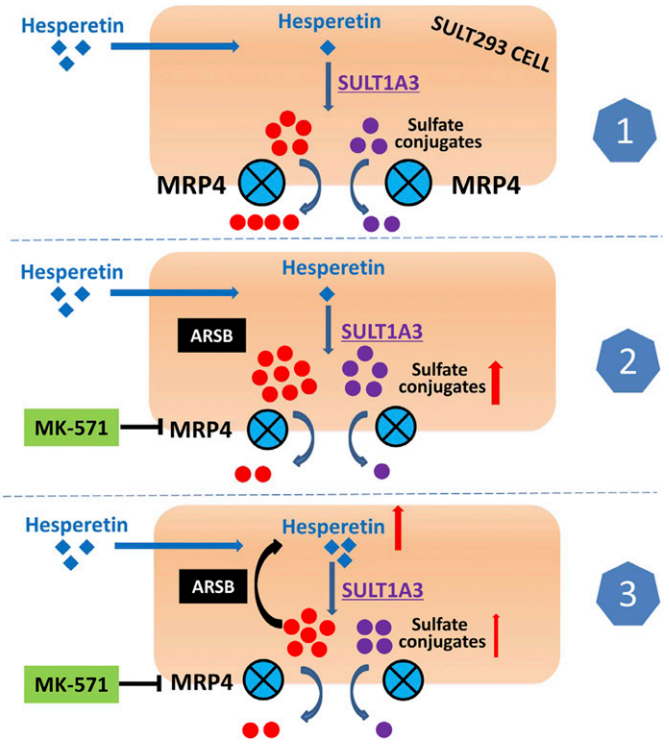

Fig. 8. A schematic representation of the underlying mechanism involved in sulfonation-transport interplay. (1) In the absence of MRP4 inhibitor, sulfated metabolites generated from hesperetin by SULT1A3 are efficiently excreted out of cells. (2) Activity suppression of efflux transporter MRP4 leads to reduced excretion of hesperetin sulfates, resulting in marked accumulation of the metabolites. (3) High levels of intracellular metabolites (as the substrates) favored the desulfonation reaction by ARSB that counteracts the metabolite formation. As a result, total cellular sulfonation is reduced. In the absence of desulfonation, metabolite formation (from the sulfonation reaction) and excretion are two independent processes. Interplay between the two processes was unlikely. The desulfonation acts to bridge the two processes. Impaired metabolite excretion resulted in its accumulation, thereby enhancing desulfonation and reducing total sulfonation.

Discussion

Drug elimination is a highly complex process that is dictated by multiple individual and interacting components (e.g., metabolism, influx, and efflux) (Benet et al., 2003). A better understanding of the intricate relationships between metabolic and transport pathways contributes to improved predictions of drug disposition in vivo (Wu and Benet, 2005). In this study, we showed that cellular sulfonation of hesperetin was significantly reduced by excretion suppression of intracellular sulfated metabolites, revealing a strong interplay of sulfonation with efflux transport. It was further unraveled that ARSB was mainly responsible for the regulatory effect of the transporter on cellular sulfonation, as evidenced by the facts that knockdown of ARSB attenuated the regulatory effect, whereas ABSB overexpression enhanced the transporter effect (Figs. 6 and 7).

It was a novel finding that ARSB played a critical role in mediating sulfonation-transport interplay. ARSB catalyzed the hydrolysis (desulfonation) of hesperetin sulfates (Fig. 4). Activity suppression of efflux transporter led to reduced excretion of hesperetin sulfates, resulting in marked accumulation of these metabolites (Fig. 2B; Fig. 8). High levels of intracellular sulfated metabolites (as the substrates) favored the desulfonation reaction by ARSB that counteracted the sulfate conjugate formation (Fig. 8). As a result, total cellular sulfonation was reduced. In the absence of desulfonation, hesperetin sulfate formation (from the sulfonation reaction) and excretion were two independent processes. Interplay between the two processes was unlikely. The desulfonation acted to bridge the two processes. Impaired sulfated metabolite excretion resulted in its accumulation, thereby enhancing desulfonation and reducing total sulfonation. The current study and our previous one highlighted that the deconjugation (or futile recycling) process was necessary for the interplay of phase II enzymes with efflux transporters to occur (Sun et al., 2015b).

The hydrolysis rate by ARSB was linear to the concentration of sulfated metabolites under test concentrations of up to 130 μM (Fig. 4), suggesting that ARSB was a low-affinity enzyme, which is consistent with the literature (Hanson et al., 2004). By contrast, the K_m values for hesperetin sulfation by SULT1A3 enzyme and SULT293 cells are around 13–15 μM, an indicator that SULT1A3 is a higher-affinity enzyme (Sun et al., 2015a). It appeared that sulfonation would be dominant due to higher SULT1A3 activity. However, this was not necessary. As intracellular metabolites accumulate (up to 12.6-fold of control) due to efflux suppression (Fig. 2B), ARSB-mediated desulfonation will be markedly enhanced as the substrate levels are greatly elevated (Fig. 8). In other words, ARSB is able to reverse sulfonation to a certain degree, affecting the total sulfonation in the cell system (Fig. 8).

Although human sulfatases constitute a number of enzymes ($n = 17$), the current study focused on ARSA, ARSB, and ARSC due to their favored activities toward small sulfate compounds (Hanson et al., 2004). Of these three enzymes, only ARSB catalyzed the desulfonation of hesperetin sulfates with an optimal reaction pH of 5.6. This was quite consistent with earlier studies in which ARSB best performed at a pH of 5.6 (Fluharty et al., 1979; Gibson et al., 1987). Accordingly, the overexpression and knockdown of ASRB were performed to pinpoint its role in the sulfonation-transport interplay.

It was discovered that the ARSB enzyme, a lysosomal protein, played a crucial role in the disposition of hesperetin through desulfonation of its sulfated conjugates. This indicated that hesperetin sulfates (hydrophilic

compounds) would require active transport into the lysosomes to be deconjugated. However, very little is known about how xenobiotic sulfates enter lysosomes. By contrast, relatively much more is known about the uptake mechanisms of inorganic sulfate into lysosomes. Lysosomal transport of inorganic sulfate is a facilitated process that is mediated by the lysosomal membrane sulfate transporter (Jonas and Jobe, 1990; Koetters et al., 1995). It remains to be determined whether hesperetin sulfates enter the lysosomes via the sulfate transporter or the organic anion uptake transporters such as organic anion transporting polypeptides. Organic anion transporting polypeptides have been shown to facilitate the transport of sulfated metabolites (e.g., resveratrol sulfate and troglitazone sulfate) into cells (Nozawa et al., 2004; Riha et al., 2014).

MK-571 was used in the present study to downregulate MRP activity to study the sulfonation-transport interplay. One significant concern regarding the application of MK-571 in the interplay study is that this inhibitor shows great potential to alter the activity of phase II enzymes. For instance, MK-571 was a mixed modifier (i.e., activation at low concentrations and inhibition at high concentrations) of UGT1A1-mediated glucuronidation of chrysin (Quan et al., 2015). MK-571 significantly inhibited glucuronidation of resveratrol by UGT1A1 through its binding to the reaction site of the enzyme (Wang et al., 2016). However, we have confirmed that MK-571 did not affect the sulfonation activity of SULT1A3 at all; thus, the reduced excretion of hesperetin sulfates was solely ascribed to the suppression of MRP transporter (Sun et al., 2015a). Therefore, MK-571 was an excellent efflux inhibitor to investigate the effects of MRPs on cellular sulfonation in SULT293 cells.

Phase II conjugation has gained increasing attention in drug discovery and development because current new chemical entities show a greater tendency to be metabolized by phase II enzymes (Rowland et al., 2013). Moreover, the first-pass metabolism by phase II enzymes limits the oral bioavailability of many drugs and active herbal-derived chemicals (Wu et al., 2011). The present study and our previous one (Sun et al., 2015b) indicated that cellular conjugation is regulated by efflux transporters. Hence, the inhibition of both enzymes and transporters represented a novel and promising strategy to enhance the oral bioavailability of drugs undergoing extensive conjugation, although the inhibition of enzyme activity alone showed potential in enhancing resveratrol bioavailability (Zhou et al., 2015).

Our study suggested that SULT293 cells were an excellent model to study the sulfonation-transport interplay, more specifically, the interplay of SUTL1A3 with MRP4. This was because SULT1A3 was the main DME expressed by the cells and MRP4 was the only transporter mediating excretion of hesperetin sulfates in the cells (Li et al., 2015; Sun et al., 2015a). It is acknowledged that the proposed simplistic interplay (between one enzyme and one transporter) remains to be verified in a more advanced system, such as Caco-2 or hepatocytes, where multiple metabolizing enzymes and multiple transporters are involved in drug disposition. However, as revealed herein, the metabolism-transport interplay was rather complex and involved additional elements such as the deconjugation system. Elucidating the simplistic interplay, as the first step, appeared to be essential toward a full understanding of and a precise prediction of the metabolism-transport interplay in vivo.

In summary, inhibited excretion of metabolites by MK-571 led to reduced metabolism of hesperetin (a maximal 78% reduction) in SULT293 cells, revealing a strong interplay of sulfonation metabolism with efflux transport. Although SULT293 cells expressed multiple sulfatases such as ARSA, ARSB, and ARSC, only ARSB showed significant activities toward hesperetin sulfates. Knockdown of ARSB attenuated the regulatory effect of the efflux transporter on cellular sulfonation, whereas ABSB overexpression enhanced the transporter effect. It was concluded that ARSB mediated the sulfonation-transport interplay in SULT293 cells.

Authorship Contributions

Participated in research design: Zhao, Wang, Li, Dong, and Wu.
Conducted experiments: Zhao, Wang, Li, and Dong.
Contributed new reagents or analytic tools: Dong.
Performed data analysis: Zhao, Wang, Dong, and Wu.
Wrote or contributed to the writing of the manuscript: Zhao, Wang, and Wu.

References

Allali-Hassani A, Pan PW, Dombrovski L, Najmanovich R, Tempel W, Dong A, Loppnau P, Martin F, Thornton J, and Edwards AM, et al. (2007) Structural and chemical profiling of the human cytosolic sulfotransferases. *PLoS Biol* **5**:e97.

Benet LZ (2009) The drug transporter-metabolism alliance: uncovering and defining the interplay. *Mol Pharm* **6**:1631–1643.

Benet LZ (2013) The role of BCS (biopharmaceutics classification system) and BDDCS (biopharmaceutics drug disposition classification system) in drug development. *J Pharm Sci* **102**:34–42.

Benet LZ, Cummins CL, and Wu CY (2003) Transporter-enzyme interactions: implications for predicting drug-drug interactions from in vitro data. *Curr Drug Metab* **4**:393–398.

Blanchard RL, Freimuth RR, Buck J, Weinshilboum RM, and Coughtrie MW (2004) A proposed nomenclature system for the cytosolic sulfotransferase (SULT) superfamily. *Pharmacogenetics* **14**:199–211.

Brand W, Boersma MG, Bik H, Hoek-van den Hil EF, Vervoort J, Barron D, Meinl W, Glatt H, Williamson G, and van Bladeren PJ, et al. (2010) Phase II metabolism of hesperetin by individual UDP-glucuronosyltransferases and sulfotransferases and rat and human tissue samples. *Drug Metab Dispos* **38**:617–625.

Brand W, van der Wel PA, Rein MJ, Barron D, Williamson G, van Bladeren PJ, and Rietjens IM (2008) Metabolism and transport of the citrus flavonoid hesperetin in Caco-2 cell monolayers. *Drug Metab Dispos* **36**:1794–1802.

Buono M and Cosma MP (2010) Sulfatase activities towards the regulation of cell metabolism and signaling in mammals. *Cell Mol Life Sci* **67**:769–780.

Chapman E, Best MD, Hanson SR, and Wong CH (2004) Sulfotransferases: structure, mechanism, biological activity, inhibition, and synthetic utility. *Angew Chem Int Ed Engl* **43**:3526–3548.

Diez-Roux G and Ballabio A (2005) Sulfatases and human disease. *Annu Rev Genomics Hum Genet* **6**:355–379.

Falany JL and Falany CN (2007) Interactions of the human cytosolic sulfotransferases and steroid sulfatase in the metabolism of tibolone and raloxifene. *J Steroid Biochem Mol Biol* **107**:202–210.

Fluharty AL, Stevens RL, Goldstein EB, and Kihara H (1979) The activity of arylsulfatase A and B on tyrosine O-sulfates. *Biochim Biophys Acta* **566**:321–326.

Freimuth RR, Wiepert M, Chute CG, Wieben ED, and Weinshilboum RM (2004) Human cytosolic sulfotransferase database mining: identification of seven novel genes and pseudogenes. *Pharmacogenomics J* **4**:54–65.

Garg A, Garg S, Zaneveld LJ, and Singla AK (2001) Chemistry and pharmacology of the Citrus bioflavonoid hesperidin. *Phytother Res* **15**:655–669.

Ghosh D (2007) Human sulfatases: a structural perspective to catalysis. *Cell Mol Life Sci* **64**: 2013–2022.

Gibson GJ, Saccone GT, Brooks DA, Clements PR, and Hopwood JJ (1987) Human N-acetylgalactosamine-4-sulphate sulphatase. Purification, monoclonal antibody production and native and subunit Mr values. *Biochem J* **248**:755–764.

Giménez-Bastida JA, González-Sarrías A, Vallejo F, Espín JC, and Tomás-Barberán FA (2016) Hesperetin and its sulfate and glucuronide metabolites inhibit TNF-α induced human aortic endothelial cell migration and decrease plasminogen activator inhibitor-1 (PAI-1) levels. *Food Funct* **7**:118–126.

Hanson SR, Best MD, and Wong CH (2004) Sulfatases: structure, mechanism, biological activity, inhibition, and synthetic utility. *Angew Chem Int Ed Engl* **43**:5736–5763.

Hempel N, Gamage N, Martin JL, and McManus ME (2007) Human cytosolic sulfotransferase SULT1A1. *Int J Biochem Cell Biol* **39**:685–689.

Jiang W, Xu B, Wu B, Yu R, and Hu M (2012) UDP-glucuronosyltransferase (UGT) 1A9-overexpressing HeLa cells is an appropriate tool to delineate the kinetic interplay between breast cancer resistance protein (BRCP) and UGT and to rapidly identify the glucuronide substrates of BCRP. *Drug Metab Dispos* **40**:336–345.

Jonas AJ and Jobe H (1990) Sulfate transport by rat liver lysosomes. *J Biol Chem* **265**: 17545–17549.

Koetters PJ, Chou HF, and Jonas AJ (1995) Lysosomal sulfate transport: inhibitor studies. *Biochim Biophys Acta* **1235**:79–84.

Lam JL, Okochi H, Huang Y, and Benet LZ (2006) In vitro and in vivo correlation of hepatic transporter effects on erythromycin metabolism: characterizing the importance of transporter-enzyme interplay. *Drug Metab Dispos* **34**:1336–1344.

Li W, Sun H, Zhang X, Wang H, and Wu B (2015) Efflux transport of chrysin and apigenin sulfates in HEK293 cells overexpressing SULT1A3: the role of multidrug resistance-associated protein 4 (MRP4/ABCC4). *Biochem Pharmacol* **98**:203–214.

Nozawa T, Sugiura S, Nakajima M, Goto A, Yokoi T, Nezu J, Tsuji A, and Tamai I (2004) Involvement of organic anion transporting polypeptides in the transport of troglitazone sulfate: implications for understanding troglitazone hepatotoxicity. *Drug Metab Dispos* **32**:291–294.

Pang KS, Maeng HJ, and Fan J (2009) Interplay of transporters and enzymes in drug and metabolite processing. *Mol Pharm* **6**:1734–1755.

Quan E, Wang H, Dong D, Zhang X, and Wu B (2015) Characterization of chrysin glucuronidation in UGT1A1-overexpressing HeLa cells: elucidating the transporters responsible for efflux of glucuronide. *Drug Metab Dispos* **43**:433–443.

Riha J, Brenner S, Böhmdorfer M, Giessrigl B, Pignitter M, Schueller K, Thalhammer T, Stieger B, Somoza V, and Szekeres T, et al. (2014) Resveratrol and its major sulfated conjugates are

substrates of organic anion transporting polypeptides (OATPs): impact on growth of ZR-75-1 breast cancer cells. *Mol Nutr Food Res* **58**:1830–1842.
Roohbakhsh A, Parhiz H, Soltani F, Rezaee R, and Iranshahi M (2015) Molecular mechanisms behind the biological effects of hesperidin and hesperetin for the prevention of cancer and cardiovascular diseases. *Life Sci* **124**:64–74.
Rowland A, Miners JO, and Mackenzie PI (2013) The UDP-glucuronosyltransferases: their role in drug metabolism and detoxification. *Int J Biochem Cell Biol* **45**:1121–1132.
Salphati L (2009) Transport-metabolism interplay. *Mol Pharm* **6**:1629–1630.
Sun H, Wang X, Zhou X, Lu D, Ma Z, and Wu B (2015a) Multidrug resistance-associated protein 4 (MRP4/ABCC4) controls efflux transport of hesperetin sulfates in sulfotransferase 1A3-overexpressing human embryonic kidney 293 cells. *Drug Metab Dispos* **43**:1430–1440.
Sun H, Zhou X, Zhang X, and Wu B (2015b) Decreased expression of multidrug resistance-associated protein 4 (MRP4/ABCC4) leads to reduced glucuronidation of flavonoids in UGT1A1-overexpressing HeLa cells: the role of futile recycling. *J Agric Food Chem* **63**: 6001–6008.
Takumi H, Nakamura H, Simizu T, Harada R, Kometani T, Nadamoto T, Mukai R, Murota K, Kawai Y, and Terao J (2012) Bioavailability of orally administered water-dispersible hesperetin and its effect on peripheral vasodilatation in human subjects: implication of endothelial functions of plasma conjugated metabolites. *Food Funct* **3**:389–398.
Wang S, Li F, Quan E, Dong D, and Wu B (2016) Efflux transport characterization of resveratrol glucuronides in UDP-glucuronosyltransferase 1A1 transfected HeLa cells: application of a cellular pharmacokinetic model to decipher the contribution of multidrug resistance-associated protein 4. *Drug Metab Dispos* **44**:485–488.
Wu B (2012) Pharmacokinetic interplay of phase II metabolism and transport: a theoretical study. *J Pharm Sci* **101**:381–393.
Wu B, Kulkarni K, Basu S, Zhang S, and Hu M (2011) First-pass metabolism via UDP-glucuronosyltransferase: a barrier to oral bioavailability of phenolics. *J Pharm Sci* **100**:3655–3681.
Wu CY and Benet LZ (2005) Predicting drug disposition via application of BCS: transport/absorption/ elimination interplay and development of a biopharmaceutics drug disposition classification system. *Pharm Res* **22**:11–23.
Yang HL, Chen SC, Senthil Kumar KJ, Yu KN, Lee Chao PD, Tsai SY, Hou YC, and Hseu YC (2012) Antioxidant and anti-inflammatory potential of hesperetin metabolites obtained from hesperetin-administered rat serum: an ex vivo approach. *J Agric Food Chem* **60**:522–532.
Zhang X, Dong D, Wang H, Ma Z, Wang Y, and Wu B (2015) Stable knock-down of efflux transporters leads to reduced glucuronidation in UGT1A1-overexpressing HeLa cells: the evidence for glucuronidation-transport interplay. *Mol Pharm* **12**:1268–1278.
Zhou J, Zhou M, Yang FF, Liu CY, Pan RL, Chang Q, Liu XM, and Liao YH (2015) Involvement of the inhibition of intestinal glucuronidation in enhancing the oral bioavailability of resveratrol by labrasol containing nanoemulsions. *Mol Pharm* **12**:1084–1095.

Address correspondence to: Baojian Wu, Division of Pharmaceutics, College of Pharmacy, Jinan University, 601 Huangpu Avenue West, Guangzhou 510632, China. E-mail: bj.wu@hotmail.com